PRAMANA
— journal of
physics

Vol. 58, No. 1
January 2002
pp. 39–57

(e, 3e) Differential cross section of He (2^1S) and He (2^3S)

KSHAMATA MUKTAVAT and M K SRIVASTAVA
Department of Physics, University of Roorkee, Roorkee 247 667, India
Email: muktadph@rurkiu.ernet.in; mksrafph@rurkiu.ernet.in

MS received 17 April 2001; revised 13 August 2001

Abstract. The angular distribution of the five-fold differential cross section for the electron impact double ionization of He (2^1S) and He (2^3S) has been studied. The kinematical conditions for maxima/minima in the angular distribution for the two cases have been compared. The two-step process for the double ionization is found to contribute very little in the triplet case.

Keywords. Angular distribution; differential cross section; electronic excitation; ionization of molecules.

PACS Nos 34.50.Fa; 34.80.Dp

1. Introduction

It is well known that the angular distribution of the five-fold differential cross section (FDCS) for the double ionization of atoms by electrons contains information about correlation between the two ejected electrons. Measurement of FDCS was first carried out about ten years ago on argon [1] and krypton [2]. The interpretation of the results and extraction of the correlation information was found to be quite difficult because besides the problems associated with double ionization mechanisms (shake-off and two-step) and proper accounting of electron–electron correlation in the final state, there are complications due to the multi-electron structure of the target and the residual ion. The position with multi-electron targets has not changed much since then [3,4]. However, recent experiments [5–7] on He have provided a fresh impetus to $(e,3e)$ studies. Helium is the simplest two-electron atom as the residual He^{2+} ion is a bare nucleus with no relevant internal structure. The details of the angular distribution of FDCS have been analysed in the coplanar geometry with symmetric and asymmetric energy sharing between the ejected electrons and in Bethe ridge kinematics [7–17]. The origin of dips and peaks in the angular distribution of the cross section has been studied [5]. The dipolar limit has been investigated and the relationship with photo-double ionization with additional non-dipolar contributions has also been noted [5,6]. The calculations have been done at large incident energy $E_0 \sim 5$ keV, very small scattering angle and low ejected electron energies corresponding to the measurements by Lahmam–Bennani and coworkers on He ground state.

In this paper we study $(e,3e)$ process on metastable para-helium He (2^1S) and ortho-helium He (2^3S) and analyse manifestation of (i) the difference in the space symmetry

of the target wave function (symmetric in He (2^1S) and antisymmetric in He (2^3S)) and (ii) the difference in binding energy of the two target electrons on the angular distribution of FDCS. We have considered both the mechanisms: the shake-off and the two-step. In the shake-off (SO) mechanism the projectile is assumed to interact only once with one of the target electrons and ejects it. The ejection of the second electron occurs subsequently through relaxation of the residual ion after the first ejection. In the symmetry breaking two-step (TS2) mechanism the incident particle interacts successively with the two target electrons ejecting them one by one and is thus a second order process in the projectile–target interaction.

2. Theory and calculations

We consider events in which electrons having energy E_0 are incident on He and are scattered inelastically into the solid angle $\mathrm{d}\Omega_a$ in the direction of (θ_a, Φ_a) and eject both the target electrons with energies E_b and E_c into the solid angle $\mathrm{d}\Omega_b$ and $\mathrm{d}\Omega_c$ in the direction of (θ_b, Φ_b) and (θ_c, Φ_c) respectively (figure 1). The FDCS for this process is given by

$$\frac{\mathrm{d}^5\sigma}{\mathrm{d}\Omega_a \mathrm{d}\Omega_b \mathrm{d}\Omega_c \mathrm{d}E_a \mathrm{d}E_b} = \frac{k_a k_b k_c}{k_0} |F|^2, \tag{1}$$

where $\vec{k}_0, \vec{k}_a, \vec{k}_b$ and $\vec{k}_c$ are the momenta of incident, scattered and ejected electrons respectively and F is the ionization amplitude. The energy and momentum conservation leads to

$$E_0 = E_a + E_b + E_c + I \tag{2}$$

and

$$\vec{k}_0 = \vec{k}_a + \vec{k}_b + \vec{k}_c + \vec{k}_r, \tag{3}$$

where I and $\vec{k}_r$ are double ionization threshold energy of the target and recoil momentum of the residual ion, respectively.

We limit ourselves to double ionization by high impact energy and the events in which the scattered electron takes away most of the energy. This enables us to describe the incident and scattered electrons by plane waves. The ionization amplitude for the shake-off and the two-step processes may be written as

$$F = f_{\mathrm{SO}} + f_{\mathrm{TS2}}. \tag{4}$$

Figure 2 shows these processes schematically. The amplitudes f_{SO} and f_{TS2} are given by [16]

$$f_{\mathrm{SO}} = -\frac{1}{2\pi} \left\langle \phi_f(\vec{r}_1, \vec{r}_2) \mathrm{e}^{i\vec{k}_a \cdot \vec{r}_0} \left| -\frac{2}{r_0} + \frac{1}{r_{01}} + \frac{1}{r_{02}} \right| \phi_0(\vec{r}_1, \vec{r}_2) \mathrm{e}^{i\vec{k}_0 \cdot \vec{r}_0} \right\rangle, \tag{5}$$

$$f_{\mathrm{TS2}} = -\frac{1}{4\sqrt{2}\pi^4} \sum_n \int \frac{\mathrm{d}\vec{q}'}{k_0^2 - k_b^2 - q'^2 + 2I_n} \left\langle \mathrm{e}^{i\vec{k}_a \cdot \vec{r}_0} \Psi^{(-)}_{C,k_c}(Z_c, \vec{r}_2) \left| \frac{1}{r_{02}} \right| \mathrm{e}^{i\vec{q}' \cdot \vec{r}_0} \phi_n(\vec{r}_2) \right\rangle$$

$$\times \left\langle e^{i\vec{q}'\cdot\vec{r}_0}\Psi^{(-)}_{C,k_b}(Z_b,\vec{r}_1)\phi_n(\vec{r}_2)\left|-\frac{2}{r_0}+\frac{1}{r_{01}}+\frac{1}{r_{02}}\right|e^{i\vec{k}_0\cdot\vec{r}_0}\phi_0(\vec{r}_1,\vec{r}_2)\right\rangle$$

$$-\frac{1}{4\sqrt{2}\pi^4}\sum_n\int\frac{d\vec{q}'}{k_0^2-k_c^2-q'^2+2I_n}\left\langle e^{i\vec{k}_a\cdot\vec{r}_0}\Psi^{(-)}_{C,k_b}(Z_b,\vec{r}_1)\left|\frac{1}{r_{01}}\right|e^{i\vec{q}'\cdot\vec{r}_0}\phi_n(\vec{r}_1)\right\rangle$$

$$\times \left\langle e^{i\vec{q}'\cdot\vec{r}_0}\Psi^{(-)}_{C,k_c}(Z_c,\vec{r}_2)\phi_n(\vec{r}_1)\left|-\frac{2}{r_0}+\frac{1}{r_{01}}+\frac{1}{r_{02}}\right|e^{i\vec{k}_0\cdot\vec{r}_0}\phi_0(\vec{r}_1,\vec{r}_2)\right\rangle, \qquad (6)$$

where

$$\phi_f(\vec{r}_1,\vec{r}_2)=\frac{1}{\sqrt{2}}\left\{\Psi^{(-)}_{C,k_b}(Z_b,\vec{r}_1)\,\Psi^{(-)}_{C,k_c}(Z_c,\vec{r}_2)\pm\Psi^{(-)}_{C,k_b}(Z_b,\vec{r}_2)\Psi^{(-)}_{C,k_c}(Z_c,\vec{r}_1)\right\} \qquad (7)$$

with + sign for double ionization of He (1^1S) and He (2^1S) and − sign for He (2^3S). $\Psi^{(-)}_{C,k}(Z,\vec{r})$ represents the Coulomb wave function given by

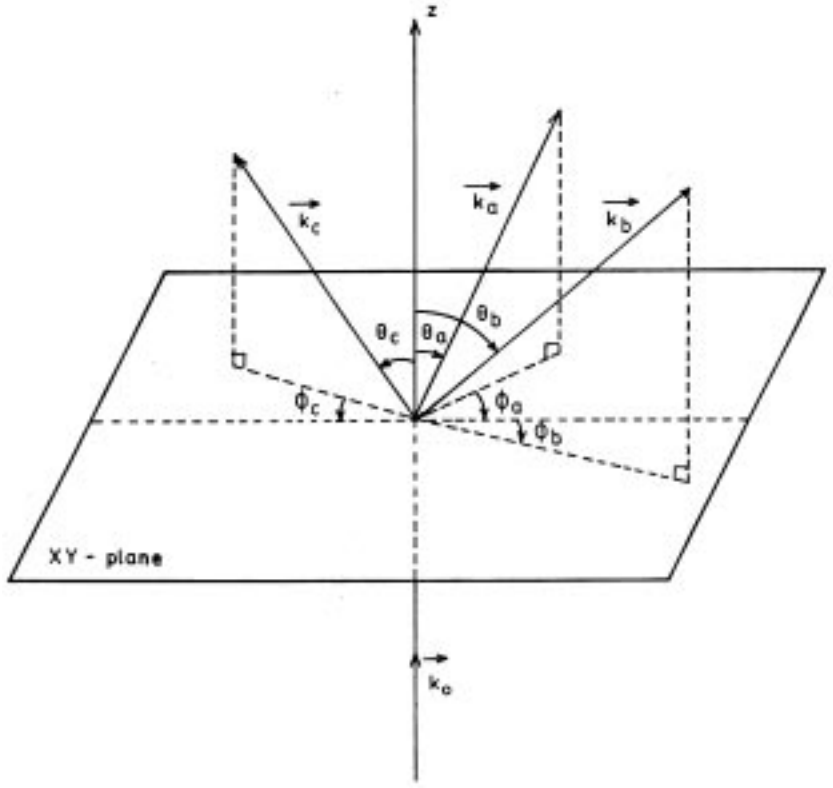

Figure 1. Schematic diagram for electron impact double ionization for an incident electron momentum $\vec{k}_0$, scattered electron momentum $\vec{k}_a$ and ejected electron momenta $\vec{k}_b$ and $\vec{k}_c$. In coplanar geometry Φ_a, Φ_b and Φ_c are such that all the electrons lie in the same plane.

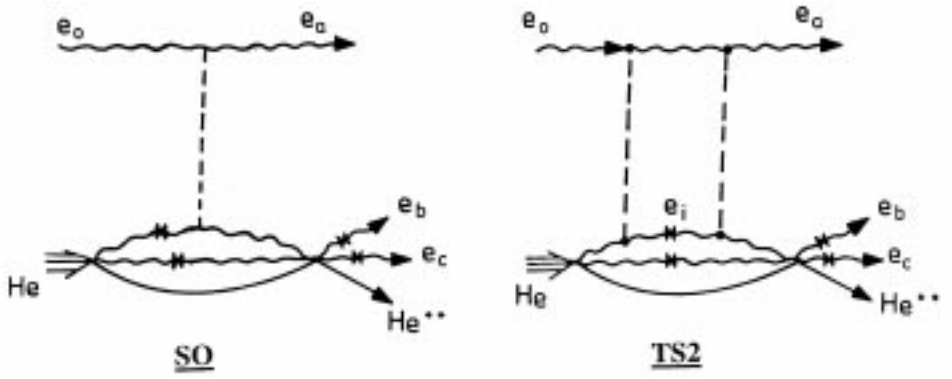

Figure 2. Schematic representation of the SO and TS2 mechanisms for the double ionization of He. The wavy line indicates an electron, dashed line the virtual photon and full line the fixed nucleus He^{++}. Crosses represent electrons in the Coulomb field of He^{++} ion.

$$\Psi^{(-)}_{C,k}(Z,\vec{r}) = \frac{1}{(2\pi)^{3/2}} e^{i\vec{k}\cdot\vec{r}}\, e^{\pi Z/2k}\Gamma(1+iZ/k)\ {}_1F_1(-iZ/k,l,-i(kr+\vec{k}\cdot\vec{r}), \quad (8)$$

where $\Gamma(1+iZ/k)$ and ${}_1F_1(-iZ/k,1,-i(kr+\vec{k}\cdot\vec{r}))$ are respectively gamma and confluent hypergeometric functions. $\phi_n(\vec{r}_2)$ is the target intermediate state wave function and $I_n = \varepsilon_0 - \varepsilon_n, \varepsilon_0$ and ε_n are the energies of ground state and intermediate state. $\phi_0(\vec{r}_1,\vec{r}_2)$ is the target initial state wave function and $\vec{r}_0, \vec{r}_1$ and $\vec{r}_2$ are the position vectors of incident and bound electrons with respect to the nucleus and $r_{01} = |\vec{r}_0 - \vec{r}_1|, r_{02} = |\vec{r}_0 - \vec{r}_2|$. The wave functions $\phi_0(\vec{r}_1,\vec{r}_2)$ for He in 1^1S, 2^1S and 2^3S states have been taken to be of the following forms [18–20]

1^1S

$$\phi_0(\vec{r}_1,\vec{r}_2) = \sum_{i=1}^{2}\gamma_i e^{-\alpha_i r_1}\sum_{j=1}^{2}\gamma_j e^{-\alpha_j r_2}; \quad \alpha_1 = 1.41, \quad \alpha_2 = 2.61,$$
$$\gamma_1 = 0.73485, \quad \gamma_2 = 0.587. \quad (9)$$

2^1S

$$\phi_0(\vec{r}_1,\vec{r}_2) = N_1\left(e^{-\mu_1 r_1}(e^{-\nu_1 r_2} + C_1 r_2 e^{-\eta_1 r_2}) + e^{-\mu_1 r_2}(e^{-\nu_1 r_1} + C_1 r_1 e^{-\eta_1 r_1})\right);$$
$$\mu_1 = 2, \quad \nu_1 = 0.865, \quad \eta_1 = 0.522, \quad N_1 = 0.9165961, \quad C_1 = -0.4327. \quad (10)$$

2^3S

$$\phi_0(\vec{r}_1,\vec{r}_2) = N_2\left(e^{-\mu_2 r_1}(e^{-\nu_2 r_2} + C_2 r_2 e^{-\eta_2 r_2}) - e^{-\mu_2 r_2}(e^{-\nu_2 r_1} + C_2 r_1 e^{-\eta_2 r_1})\right);$$
$$\mu_2 = 2, \quad \nu_2 = 1.57, \quad \eta_2 = 0.61, \quad N_2 = 1.0489/\pi, \quad C_2 = -0.34. \quad (11)$$

These wave functions have also been used earlier in inelastic scattering studies on He [21–24].

Assuming that the ejected electron completely shields the charge of the nucleus seen by the other electron, the effective charge of the nucleus seen by the two ejected electrons is chosen to be unity. It is not a bad choice as the two electrons are very slow and ejected with the same energy and are therefore in quite close proximity to the nucleus during the process. Other momentum-dependent choices [6,7,14] have not been used, as our aim in the present paper is to compare the He (2^3S) and He (2^1S) results with those for the ground state. The term f_{TS2} is evaluated using the method of Byron and Joachain [25] by replacing I_n by the average excitation energy and then using closure property of target states. The final state wave function is multiplied by the repulsive Gamow factor N_{ee},

$$N_{ee} = \mathrm{e}^{-\pi/2k_{bc}}\Gamma(1 - i/k_{bc}) \tag{12}$$

to approximate the BBK wave function [26]. This approximation to the BBK wave function has been used earlier [27–29] and is found to lead to essentially identical relative magnitude and angular distribution.

3. Results and discussion

We have carried out calculations in the coplanar geometry ($\vec{k}_0, \vec{k}_a, \vec{k}_b$ and $\vec{k}_c$ are in the same plane) at an incident energy $E_0 = 5.6$ keV and scattering angle $\theta_a = 0.45^\circ$, which correspond to the recent measurements of Lahmam-Bennani *et al* [5,6], for a variety of kinematical conditions. These are:

(A) The two ejected electrons share equal energy, $E_b = E_c$, and one of them is ejected along the momentum transfer direction, $\theta_b = \theta_q$. The angle θ_c is varied.

(B) The two electrons share equal energy and one of them is ejected in a direction perpendicular to that of momentum transfer, $\theta_b = \theta_q - 90^\circ$. The angle θ_c is varied.

(C) For both the above kinematical arrangements as well as for $\theta_b = \theta_q - 180^\circ$, we have also considered separately the direct ejection of one of the electrons, say b from $n = 1$ or $n = 2$ orbital of He, along a fixed direction while the other one, say c, is ejected through shake-off.

(D) The angle $\theta_{bc} = \theta_b - \theta_c$ between the two ejected electrons is kept fixed with $E_b = E_c$ and θ_c is varied.

(E) Symmetrical variation of the direction of ejection of both the secondary electrons with respect to the momentum transfer direction, i.e., $\theta_{bq} = \theta_{cq}$ and $|\Phi_{bq} - \Phi_{cq}| = \pi$, where $\theta_{bq}, \Phi_{bq}, \theta_{cq}$ and Φ_{cq} are the angles of the ejected electrons measured from the momentum transfer direction.

(F) Bethe ridge kinematics with fixed $E_b + E_c$. The angle θ_{bc} is varied.

(G) Bethe ridge kinematics with $E_b = E_c$, $\theta_{bq} = \theta_{cq}$ and $|\Phi_{bq} - \Phi_{cq}| = \pi$ for a fixed value of q. The angle θ_a is varied.

Kinematics A

Figure 3 shows FDCS for $\theta_b = \theta_q, E_b = E_c = 10$ eV as a function of θ_c. The momentum transfer direction θ_q is 319° for the He ground state (GS) and $\sim 312^\circ$ for the singlet

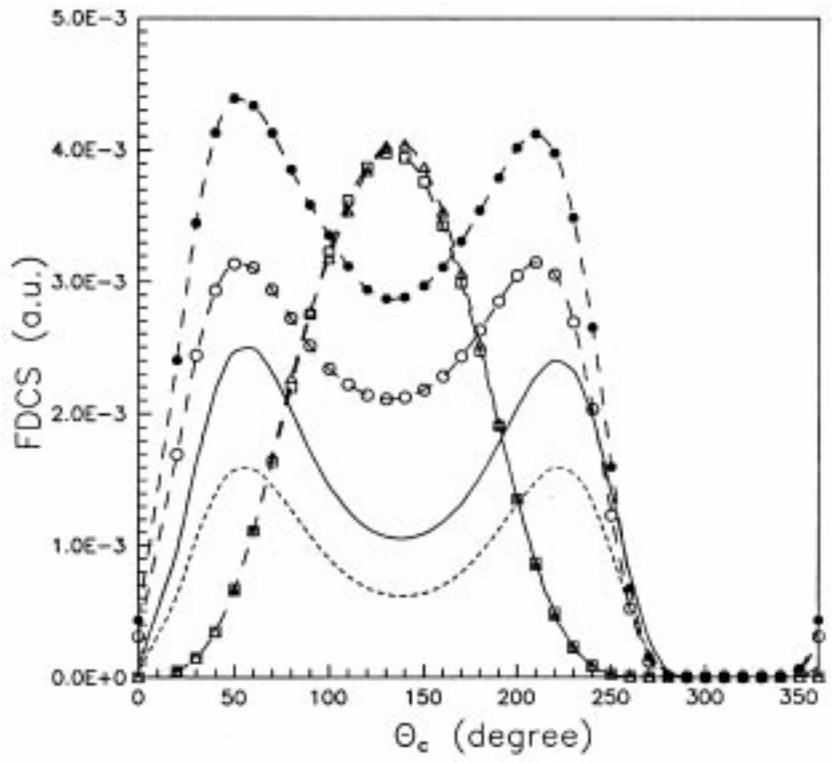

Figure 3. Coplanar FDCS (in a.u.) for the double ionization of He at $E_0 = 5.6$ keV, $\theta_a = 0.45°$ plotted against θ_c. The azimuthal angle Φ_c is fixed as zero. The ejected electrons are detected with equal energies $E_b = E_c = 10$ eV. One of the electrons b is fixed in the direction of momentum transfer $\hat{q}$, i.e. $\theta_b = \theta_q$. The solid and the dashed lines are the results for He (1^1S) with TS2 and without TS2 respectively. The dashed lines with filled circles, empty circles, triangles and squares represent results for He (2^1S) with TS2, He (2^1S) without TS2, He (2^3S) with TS2 and He (2^3S) without TS2, respectively.

2^1S (SES) and triplet 2^3S (TES) excited states. The cross section naturally vanishes in all cases when the two ejected electrons are emitted along the same direction. For TES, the FDCS shows only one lobe with maximum along $\theta_c = \theta_q + 180°$. On the other hand, for GS and SES the FDCS shows a two equal sized lobe structure with maxima at about $\pm 90°$ and minimum along $\theta_c = \theta_q + 180°$. This difference is due to different space symmetry of the singlet and triplet wave functions. The SES and TES peak cross sections are found to be much larger compared to GS. This is a reflection of smaller ionization potential in SES and TES cases. The contribution of the TS2 process is found to be quite high (about 50% of SO) in the case of GS and SES, whereas it is negligible in the case of TES.

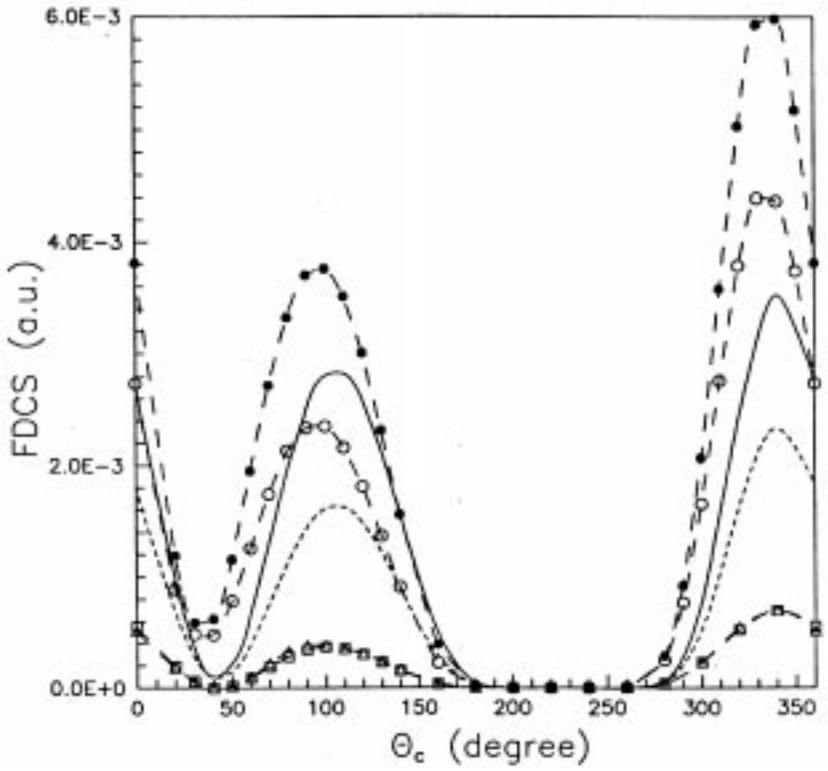

Figure 4. Same as figure 3, but for $\theta_b = \theta_q - 90^\circ$.

Kinematics B

The angular variation in this kinematics $(\theta_b = \theta_q - 90^\circ)$ has similar qualitative behavior for all the three cases GS, SES and TES (figure 4). The symmetry of the wave function produces no qualitative change in the angular variation. It shows two maxima and two minima. The minima are at $\theta_c = \theta_b$ and $\theta_b + 180^\circ$ and the maximum closer to the direction of $\vec{q}$ is of larger magnitude compared to the other one. The cross section peak is lowest for TES, while it is maximum for SES. Here again TS2 contributes very little in the TES case.

Kinematics C

Here we consider results for direct ejection of an electron, say b, from either $n = 1$ or $n = 2$ orbital with the other electron being ejected by SO for SES and TES. The direction of ejection θ_b is kept fixed at θ_q (figure 5a), $\theta_q - 90^\circ$ (figure 5b) and $\theta_q - 180^\circ$ (figure 5c) and the results are studied as a function of θ_c for TES. Figures 6a–c similarly display results for SES. It is found that $n = 1$ and $n = 2$ results in the TES case are qualitatively similar and

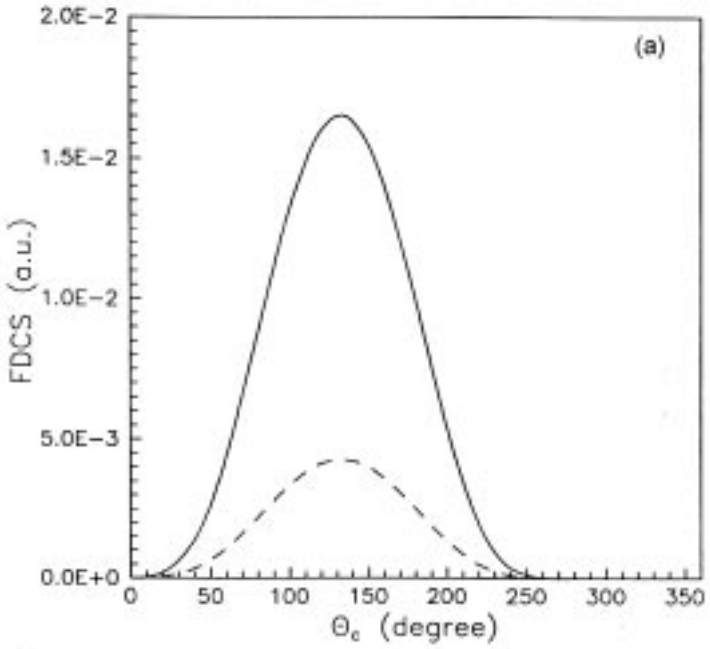

Figure 5a.

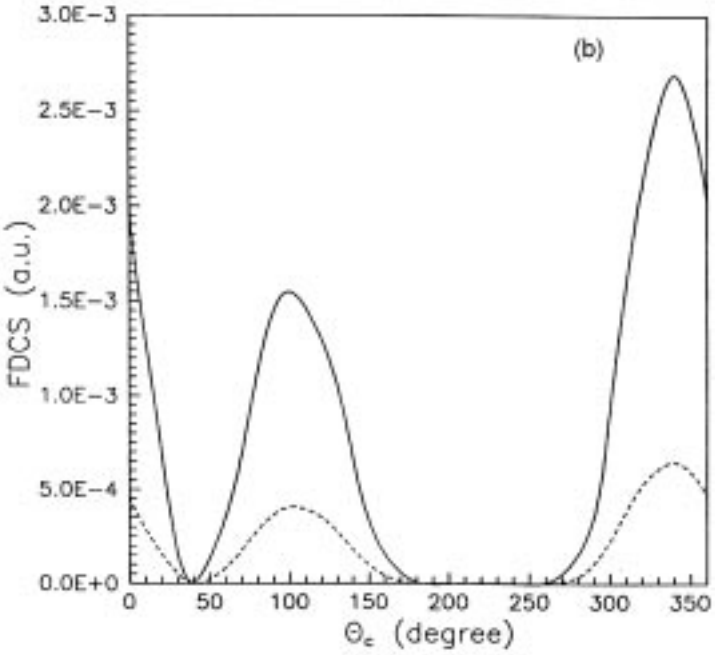

Figure 5b.

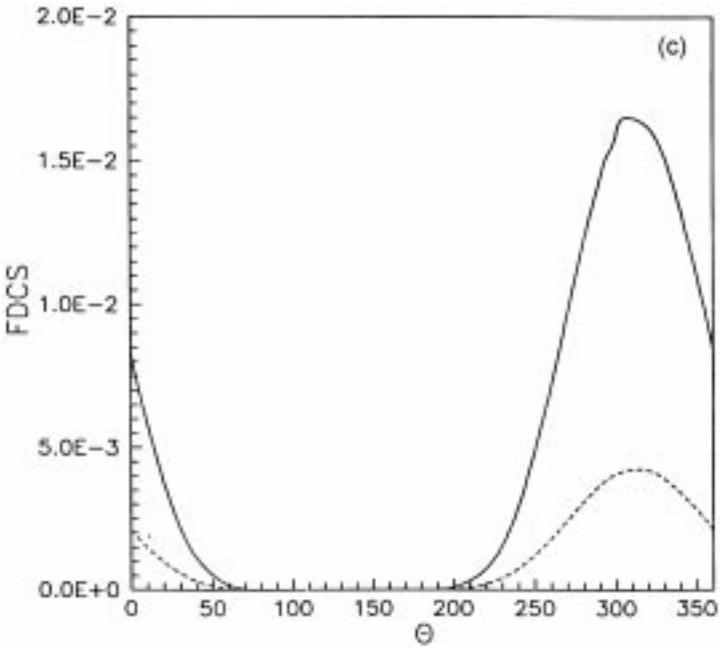

Figure 5. Coplanar FDCS (in a.u.) plotted against θ_c for He (2^3S). $E_0 = 5.6$ keV, $\theta_a = 0.45°$, $E_b = E_c = 10$ eV, the dashed line represents the results when electron b is directly ejected from $n = 1$ and the other electron is ejected by shake-off and the solid line when electron b is directly ejected from $n = 2$ and the other electron c is ejected by shake-off. The direction of ejection of directly ejected electron θ_b is fixed at (**a**) θ_q, (**b**) $\theta_q - 90°$ and (**c**) $\theta_q - 180°$.

it does not matter whether the direct ejection is from $n = 1$ or $n = 2$ orbital. The cross section peak for direct emission from $n = 2$ orbital is about four times the value for direct emission from $n = 1$. However, in the SES case (figures 6a–c), the situation is different. The angular variation depends on whether the direct ejection is from $n = 1$ or $n = 2$ orbital. Direct emission from $n = 1$ leads to a one-lobe structure in all the three kinematical conditions. In the case of direct emission from $n = 2$ orbital, there are two maxima (figure 6b) or three maxima (figure 6c) in the angular distribution. Another difference is that this peak value for $n = 2$ is not necessarily greater than the one for $n = 1$. This difference in the angular variation is a reflection of the difference in space-symmetry of the target wave function in the two cases.

Kinematics D

Figures 7a–c show the variation of FDCS for fixed $\theta_{bc} = 60°, 120°$ and $180°$ respectively. The cross section shows a maximum whenever the two electrons are ejected symmetrically with respect to the momentum transfer direction in the case of GS and SES. This happens when both θ_b and θ_c make angles of $30°$ and $150°$ with $\hat{q}$ (figure 7a) and $60°$ and $120°$

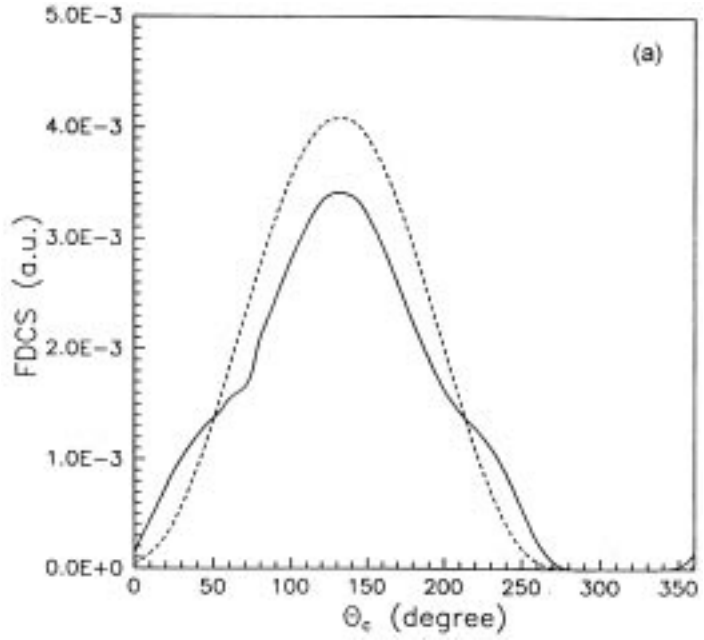

Figure 6a.

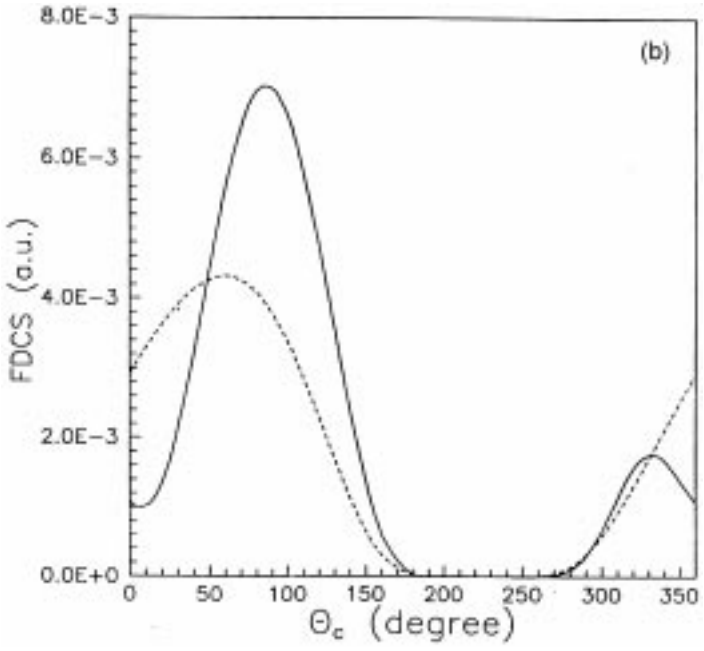

Figure 6b.

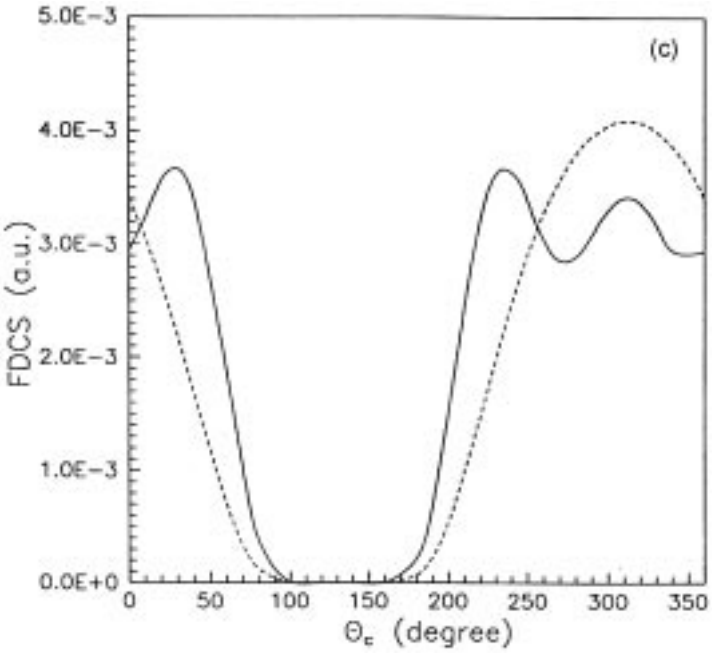

Figure 6. Same as figure 5, but for He (2^1S).

with $\hat{q}$ (figure 7b). The result is a two-lobe structure. In the TES case, symmetric ejection with respect to $\hat{q}$ corresponds to minima. Here maximum in FDCS occurs when $\vec{k}_b$ and $\vec{k}_c$ make supplementary angles with $\hat{q}$. The minima occur at $\theta_c = 20^\circ (\theta_b = 80^\circ)$ and 200° $(\theta_b = 260^\circ)$ (figure 7a). Both these values correspond to $(\theta_b + \theta_c)/2 = 90^\circ$ with respect to $\hat{q}$. When $\theta_{bc} = 180^\circ$ (figure 7c), symmetrical ejection lead to a four-lobe structure with maxima at $\theta_c = 0^\circ, 90^\circ, 180^\circ$ and 270° with respect to $\hat{q}$. Those at 90° and 270° are smaller and vanish in the dipole limit.

Kinematics E

Figure 8 shows results for symmetrical ejection with respect to the momentum transfer direction. TES does not contribute to this case. This is an interesting display of the space antisymmetric nature of the TES wave function. The GS and SES results are qualitatively similar and show a two-lobe structure with zero cross section for $\theta_b = \theta_c = 0^\circ, \theta_b = \theta_c = 180^\circ$ (identical directions) and maxima for $\theta_b = \theta_c = 100^\circ$ and 240°. SES cross sections are larger as before. The TS2 contribution is quite high. It is about 46% and 34% at the peaks of GS and SES results.

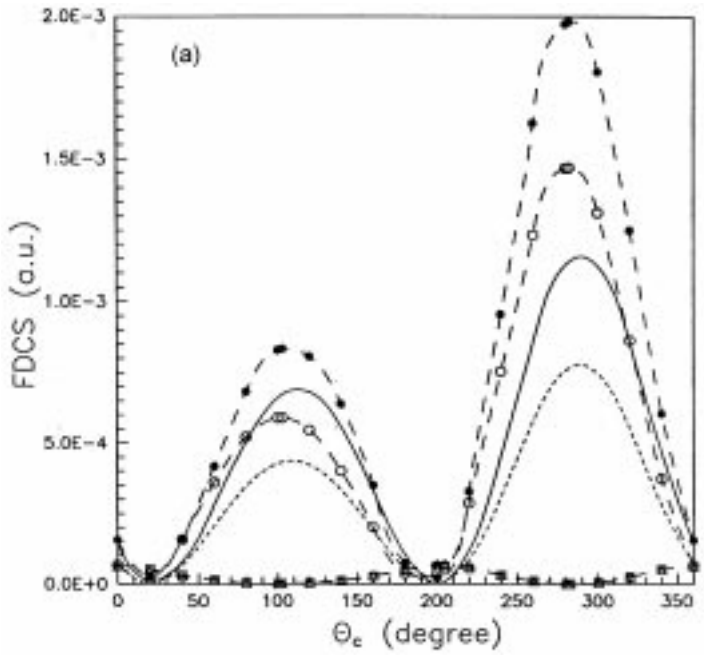

Figure 7a.

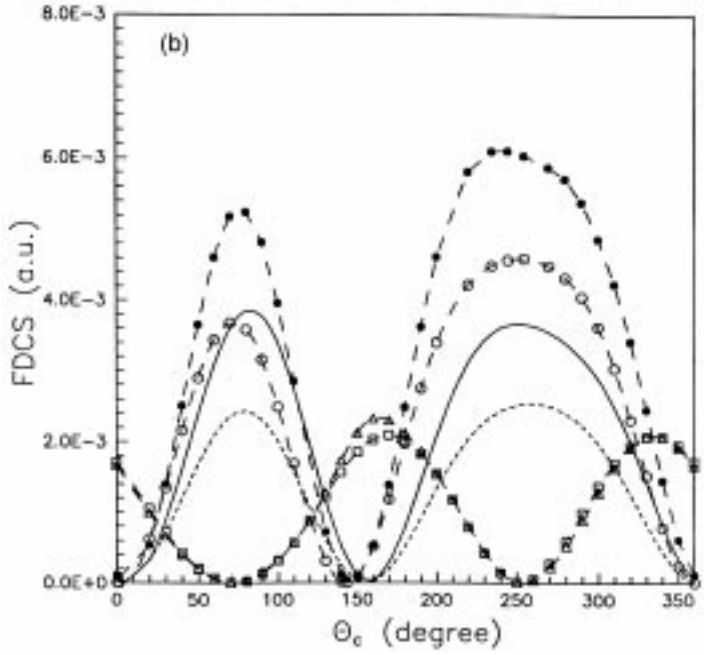

Figure 7b.

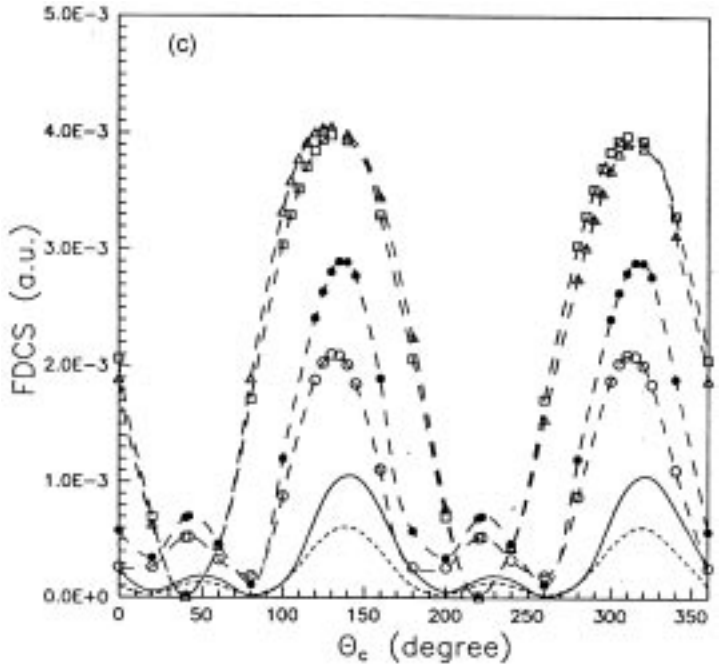

Figure 7. Same as figure 3, but the angle θ_c is varied keeping the angle between the two ejected electrons $\theta_{bc} = \theta_b - \theta_c$ fixed at (**a**) 60°, (**b**) 120° and (**c**) 180°.

Kinematics F

The Bethe ridge kinematics corresponds to the case when no momentum is transferred to the residual ion $(\vec{k}_r = 0)$. The energy–momentum conservation equations are now

$$E_0 - I - E_a = E_b + E_c, \tag{13}$$

$$\vec{k}_0 - \vec{k}_a = \vec{q} = \vec{k}_b + \vec{k}_c. \tag{14}$$

At a given incident energy E_0 and fixed energy E_a of the scattered electron (fixed $E_b + E_c$) and fixed scattering angle θ_a (or momentum transfer $\vec{q}$), the above equations can be solved for E_b and E_c These values naturally depend on the angle θ_{bc}. These equations may be solved under several conditions. If one of the electrons is assumed to be ejected with low energy along the momentum transfer direction, and the other with still lower energy along the opposite direction, the values of E_b and E_c for a given $E_b + E_c$ may be obtained. Now as the angle θ_{bc} is varied from 180° to lower values, E_b, E_c, θ_b and θ_c may be obtained up to some minimum value of θ_{bc} (tables 1 and 2). The FDCS for $(e,3e)$ on He (1^1S) for this kinematics have been studied by Srivastava *et al* [14]. Figures 9a and b shows our results for $E_b + E_c = 4$ eV and 10 eV. The TES results show a peak at $\theta_{bc} = 180°$ as in kinematics A and decrease monotonically with decrease in θ_{bc}. TS2 contribution is

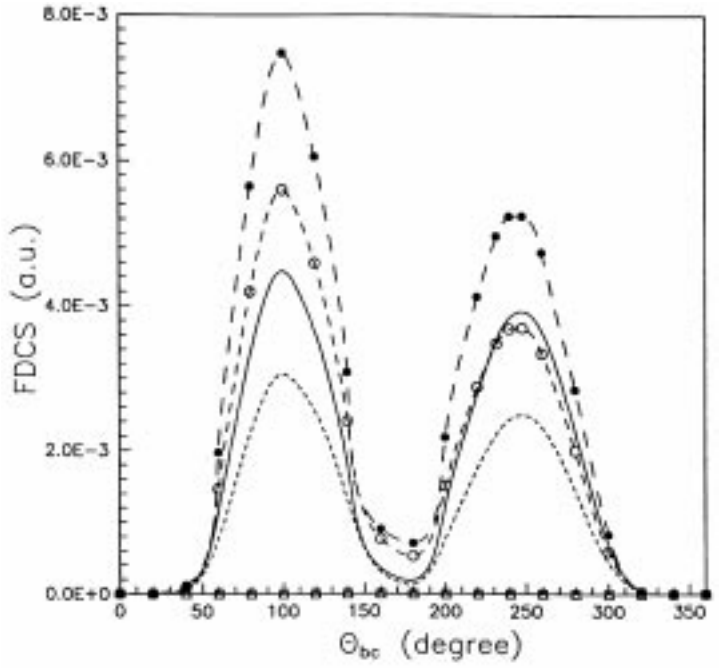

Figure 8. Angular distribution of FDCS when the angle between the two ejected electrons is varied symmetrically with respect to the momentum transfer direction. $E_0 = 5.6$ keV, $\theta_a = 0.45°$, $E_b = E_c = 10$ eV, $\theta_{bq} = \theta_{cq}$, $|\Phi_{bq} - \Phi_{cq}| = \pi$. Description of the lines is same as in figure 3.

Table 1. Values of E_b and θ_{bq} in Bethe ridge condition $(\vec{k}_r = 0)$ for fixed incident energy $E_0 = 5.6$ keV and $\theta_a = 0.45°$, for a fixed value of $E_b + E_c = 4$ eV and at different values of θ_{bc} $(\theta_{bc} = \theta_{bq} - \theta_{cq}, |\Phi_{bq} - \Phi_{cq}| = \pi)$.

	For He (1^1S)		For He (2^1S)		For He (2^3S)	
$\theta_{bc}(°)$	E_b (eV)	$\theta_{bq}(°)$	E_b (eV)	$\theta_{bq}(°)$	E_b (eV)	$\theta_{bq}(°)$
180	3.095	0	2.984	0	2.987	0
175	3.085	5.92	2.972	7.05	2.975	7.03
170	3.054	12.06	2.935	14.41	2.938	14.37
165	2.999	18.70	2.866	22.50	2.870	22.43
160	2.909	26.24	2.753	32.04	2.757	31.92
155	2.768	35.50	2.557	44.87	2.561	44.64
150	2.514	48.98	–	–	–	–

small as in other kinematical arrangements and vanishes at $\theta_{bc} = 180°$. The SES results are lower as expected and peak at smaller θ_{bc}. The GS results are lowest and show an almost flat variation over the possible range of θ_{bc}.

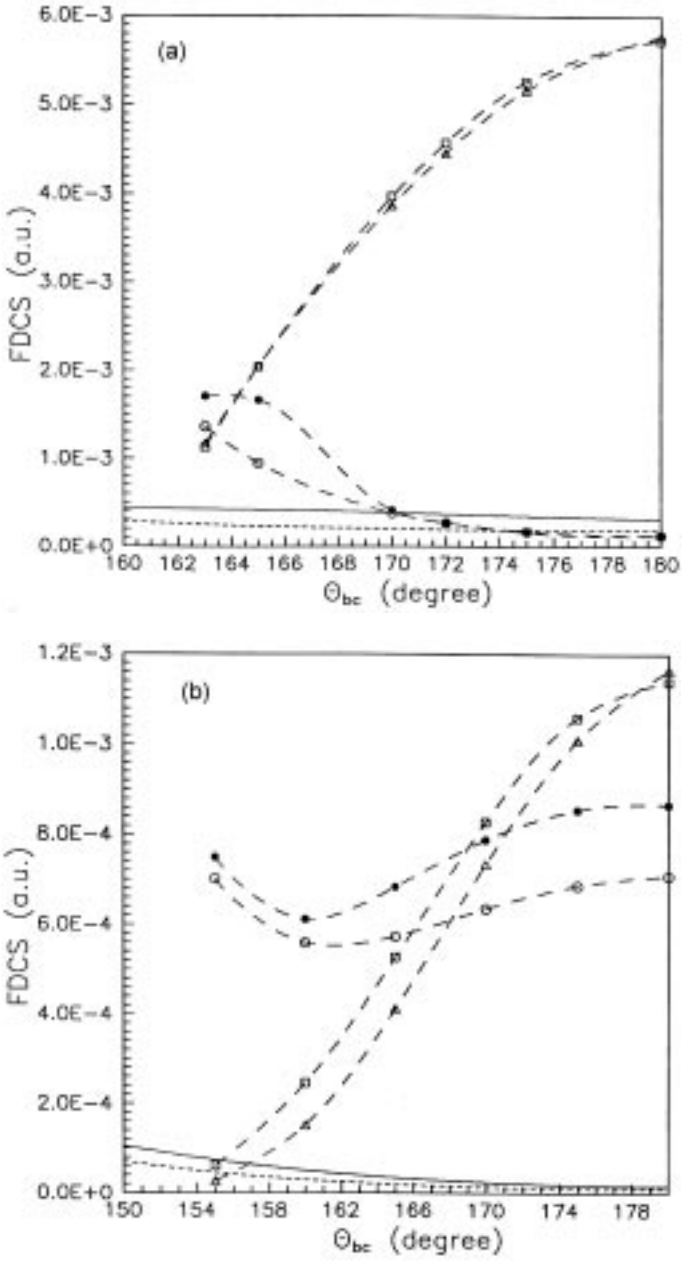

Figure 9. Coplanar FDCS (in a.u.) plotted against θ_{bc}. $E_0 = 5.6$ keV, $\theta_a = 0.45°$, E_b, E_c, θ_b and θ_c are such that Bethe ridge condition $(\vec{k}_r = 0)$ is satisfied at all values of θ_{bc}. $E_b + E_c$ is fixed at (**a**) 4 eV and (**b**) 10 eV. Description of the lines is same as in figure 3.

Table 2. Values of E_b and θ_{bq} in Bethe ridge condition ($\vec{k}_r = 0$) for fixed incident energy $E_0 = 5.6$ keV and $\theta_a = 0.45°$, for a fixed value of $E_b + E_c = 10$ eV and at different values of $\theta_{bc}(\theta_{bc} = \theta_{bq} - \theta_{cq}, |\Phi_{bq} - \Phi_{cq}| = \pi)$.

	For He (1^1S)		For He (2^1S)		For He (2^3S)	
$\theta_{bc}(°)$	E_b (eV)	$\theta_{bq}(°)$	E_b (eV)	$\theta_{bq}(°)$	E_b (eV)	$\theta_{bq}(°)$
180	6.836	0	6.639	0	6.645	0
175	6.791	10.76	6.586	12.51	6.593	12.44
170	6.643	22.36	6.412	26.26	6.419	26.12
165	6.349	36.26	6.041	43.85	6.052	43.55
160	5.712	57.89	–	–	–	–

Table 3. Values of E_b, E_c, $\theta_{bq} = \theta_{cq}$ $(|\Phi_{bq} - \Phi_{cq}| = \pi)$ in Bethe ridge condition ($\vec{k}_r = 0$) for fixed incident energy $E_0 = 5$ keV and fixed magnitude of momentum transfer $q = 0.4313$ a.u. at different values of θ_a.

	For He (1^1S)		For He (2^1S)		For He (2^3S)	
$\theta_a(°)$	$E_b = E_c$ (eV)	$\theta_{bq} = \theta_{cq}(°)$	$E_b = E_c$ (eV)	$\theta_{bq} = \theta_{cq}(°)$	$E_b = E_c$ (eV)	$\theta_{bq} = \theta_{cq}(°)$
0.3	68.76	84.50	79.07	84.87	78.67	84.86
0.4	66.40	84.40	76.71	84.79	76.31	84.78
0.5	63.28	84.26	73.59	84.68	73.19	84.67
0.6	59.33	84.07	69.63	84.53	69.24	84.52
0.7	54.42	83.81	64.72	84.33	64.33	84.31
0.8	48.39	83.44	58.70	84.04	58.30	84.02
0.9	40.98	82.86	51.28	83.62	50.89	83.60
1.0	31.71	81.88	42.02	82.95	41.62	82.92
1.1	19.69	79.68	30.00	81.65	29.60	81.60

Kinematics G

In this arrangement a symmetric solution ($E_b = E_c, \theta_{bq} = \theta_{cq}, |\Phi_{bq} - \Phi_{cq}| = \pi$) of eqs (13) and (14) is obtained for fixed $\vec{q}$. The scattering angle θ_a naturally varies. Table 3 gives the values of E_b and θ_b for different θ_a. Figure 10 shows variation of FDCS. The GS results are found to be larger than SES ones. Both increase with increasing θ_a. This is because of smaller values of $E_b(= E_c)$ in the case of GS. This being a symmetric kinematics, FDCS for TES vanishes.

4. Conclusions

We have compared FDCS for the $(e,3e)$ process on He (1^1S), He (2^1S) and He (2^3S) at an incident energy of 5.6 keV and scattering angle of 0.45° in the coplanar geometry in a variety of kinematical situations. It has been assumed that most of the energy is carried away by the scattered electron. The process is nearly dipolar. Equal energy sharing

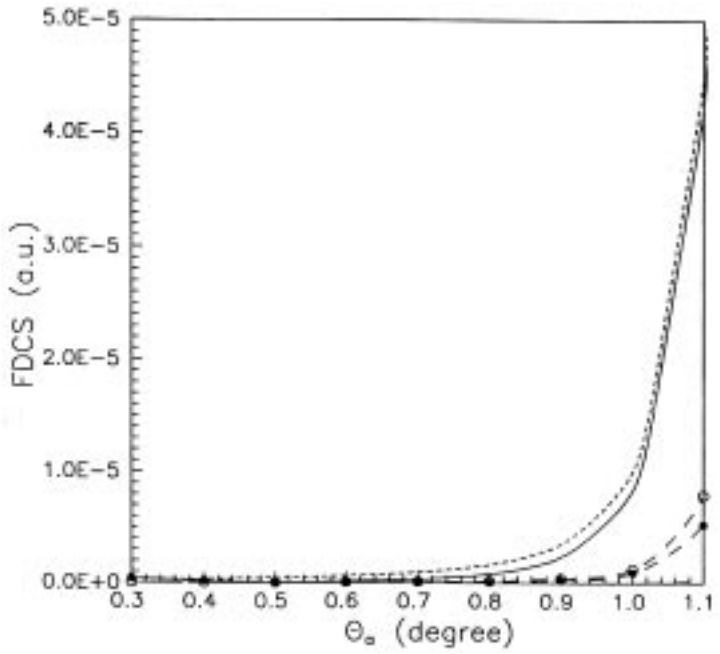

Figure 10. Coplanar FDCS (in a.u.) plotted against θ_a. $E_0 = 5$ keV, $E_b = E_c$, $\theta_{bq} = \theta_{cq}$ and $|\Phi_{bq} - \Phi_{cq}| = \pi$ are such that Bethe ridge conditions are satisfied at all values of θ_a for a fixed value of momentum transfer q. Description of the lines is same as in figure 3.

between the two ejected electrons has been considered except in Bethe ridge kinematics where $E_b + E_c$ is held constant.

It is found that the angular distribution of FDCS depends, besides the target wave function and the *e–e* correlation therein, mainly on the mutual repulsion between the two ejected electrons in the final state (approximately incorporated by the Gamow factor) and the symmetry of the target wave function. The Gamow factor leads to a peak in the cross section at $\theta_{bc} = \pi$. The angular distribution near the peak is given by $e^{-\pi\alpha^2/8k}$ where α is the deviation from the peak. The symmetry of the target wave function leads to a dependence

$$[(\vec{k}_b + (-1)^{(S-1)/2}\vec{k}_c) \cdot \vec{q}]^2$$

or

$$[\cos(\theta_b - \theta_q) + (-1)^{(S-1)/2}\cos(\theta_c - \theta_q)]^2 \tag{15}$$

for fixed k_b, k_c and q near the dipole limit. S is the multiplicity of the wave function. The condition

$$(\theta_{b,c} - \theta_q) = \pm\pi/2 \tag{16}$$

leads to minimum both for the singlet and as well as triplet cases (kinematics B). For the singlet wave function this reduces to [7]

$$[\cos(\theta_b - \theta_q) + \cos(\theta_c - \theta_q)]^2. \tag{17}$$

Equation (17) leads to a minimum in the cross section at [6]

$$\vec{k}_b = -\vec{k}_c, \tag{18}$$

$$(\vec{k}_b + \vec{k}_c) \perp \vec{q}. \tag{19}$$

For the triplet wave function eq. (15) leads to a minimum at

$$\vec{k}_b \cdot \vec{q} = \vec{k}_c \cdot \vec{q}, \tag{20}$$

i.e. symmetrical ejection with respect to the momentum transfer direction. Kinematics E corresponds to this case. Opposite directions of ejection ($\vec{k}_b = -\vec{k}_c$) lead to a maximum in the triplet case whereas in the singlet case they lead to a minimum. This minimum will naturally be shallower if $E_b \neq E_c$.

The study and analysis of kinematics C results show that the shake-off proceeds in two ways. The other ejected electron feels the effect of the direct ejection in the close vicinity and the overall effect of relaxation of the system after the direct ejection. The former effect is much weaker in the TES case leading to qualitatively similar behavior in the two cases (direct emission from $n = 1$ or 2) and larger peak cross section in the case of direct emission from $n = 2$ orbital because of smaller ionization potential.

The contribution from the two-step process in all kinematical arrangements considered here is found to be very little in the triplet case. When the projectile ejects one of the electron, there is very small probability in this case for the scattered electron in the intermediate state to find the other electron in the close vicinity because of the antisymmetry of the target wave function, so that it could be able to eject it.

Acknowledgements

This work was supported by the Department of Science and Technology, Government of India under their thrust area program. One of us (KM) would like to thank DST for the award of a research fellowship.

References

[1] A Lahmam-Bennani, C Dupre and A Duguet, *Phys. Rev. Lett.* **63**, 1582 (1989)
[2] A Lahmam-Bennani, A Duguet, A M Grisogono and M Lecas, *J. Phys.* **B25**, 2873 (1992)
[3] B E Marji, C Schröter, A Duguet, A Lahmam-Bennani, M Lecas and L Spielberger, *J. Phys.* **B30**, 3677 (1997)
[4] C Schröter, B E Marji, A Lahmam-Bennani, A Duguet, M Lecas and L Spielberger, *J. Phys.* **B31**, 131 (1998)
[5] I Taouil, A Lahmam-Bennani, A Duguet and L Avaldi, *Phys. Rev. Lett.* **81**, 4600 (1998)

[6] A Lahmam-Bennani, I Taouil, A Duguet, M Lecas, L Avaldi and J Berakdar, *Phys. Rev.* **A59**, 3548 (1999)
[7] A Kheifets, I Bray, A Lahmam-Bennani, A Duguet and I Taouil, *J. Phys.* **B32**, 5047 (1999)
[8] C Dal Cappello and H Le Rouzo, *Phys. Rev.* **A43**, 1395 (1991)
[9] B Joulakian, C Dal Cappello and M Brauner, *J. Phys.* **B25**, 2863 (1992)
[10] R J Tweed, *Z. Phys*. **D23**, 309 (1992)
[11] B Joulakian and C Dal Cappello, *Phys. Rev.* **A47**, 3788 (1993)
[12] J Berakdar and H Klar, *J. Phys.* **B26**, 4219 (1993)
[13] P Lamy, B Joulakian, C Dal Cappello and A Lahmam-Bennani, *J. Phys.* **B29**, 2315 (1996)
[14] M K Srivastava, S Gupta and C Dal Cappello, *Phys. Rev.* **A53**, 4104 (1996)
[15] C Dal Cappello, R E Mkhanter and P A Hervieux, *Phys. Rev.* **A57**, 693 (1998)
[16] R E Mkhanter and C Dal Cappello, *J. Phys.* **B31**, 301 (1998)
[17] M Grin, C Dal Cappello, R E Mkhanter and J Rasch. *J. Phys.* **B33**, 131 (2000)
[18] F W Byron Jr. and C J Joachain, *Phys. Rev.* **146**, 1 (1966)
[19] F W Byron Jr. and C J Joachain, *J. Phys.* **B8**, L284 (1975)
[20] G A Khayrallah, S T Chen and J R Rumbell Jr., *Phys. Rev.* **A17**, 513 (1978)
[21] G P Gupta and K C Mathur, *J. Phys.* **B12**, 1733 (1979)
[22] G P Gupta and K C Mathur, *Phys. Rev.* **A22**, 1455 (1980)
[23] S Saxena, G P Gupta and K C Mathur, *Indian J. Phys.* **B57**, 154 (1983)
[24] S Saxena, G P Gupta and K C Mathur, *Phys. Rev.* **A27**, 225 (1983)
[25] F W Byron Jr. and C J Joachain, *Phys. Rev.* **A8**, 1267 (1973)
[26] M Brauner, J S Briggs and H Klar, *Z. Phys.* **D11**, 257 (1989)
[27] C Dal Cappello and B Joulakian, in $(e,2e)$ and Related Processes 1993, *Proceedings of the NATO Advanced Research Workshop*, edited by C T Whelan (Cambridge, 1992)
[28] J Botero and J H Macek, *Phys. Rev. Lett.* **68**, 576 (1991)
[29] C T Whelan, R J Allan, J Rasch, H R J Walters, X Zhang, J Roder, K Jung and H Ehrhardt, *Phys. Rev.* **A50**, 4394 (1994)